INTEGRATING GPR AND CCRI TECHNIQUES: IMPLICATIONS FOR IDENTIFYING AND MAPPING NEAR-SURFACE GROUND ICE ON MARS.

J-M. Wan Bun Tseung, P. A. Wainstein, B. J. Moorman, C. W. Stevens, and C. H. Hugenholtz. Department of Geography, University of Calgary, 2500, University Drive N.W., Calgary, Alberta, T2N 1N4, Canada. Email: jm.wanbt@ucalgary.ca

Introduction: Since the early flyby missions of the 1960s, the study of Mars has largely focused on the discovery of exploitable water for future manned missions. Data generated by the Mars Odyssey neutron and gamma-ray spectrometers indicate large reservoirs of hydrogen (possibly H_2O ice) in the near-surface of Mars at latitudes greater than 50° [1], [2], [3]. Additionally, Viking orbiters and the Mars Orbiter Camera have revealed numerous landforms, possibly related to ground ice and permafrost processes (e.g. polygonal terrain, pingo-like mounds, thermokarst depressions, debris-aprons, and rock glacier-like features). However, despite observational evidence, an accurate identification and mapping of near-surface ground ice remains an open research question.

As such, the use of geophysical methods for investigating the Martian subsurface has witnessed growing interest among planetary scientists. Research involving the design and testing of geophysical instruments has focused primarily on seismic sounding (e.g. [4]), Time Domain Electromagnetic and Surface Nuclear Magnetic Resonance sounding [5] and GPR [6], [7], [8], [9], [10]. Within the context of these earlier studies, the purpose of this research is to combine GPR and Capacitively Coupled Resistivity Imaging (CCRI) systems to image ground ice and subsurface structures in a proglacial environment analogous to terrain types thought to exist on Mars.

Whereas GPR measures the reflections of high-frequency electromagnetic (EM) waves to image the dielectric changes within the subsurface, CCRI uses an electric current to image electrical resistivity changes at depth.

Study site: The Athabasca Glacier in Alberta, Canada (fig.1) provides access to a variety of terrain types including proglacial till deposits, fine to coarse glacio-fluvial sediments, buried and exposed bedrock, bouldery surfaces, as well as terrain with different ice contents ranging from massive buried ice (ice-cored moraine and debris-covered glacier ice) to interstitial ice. Similar terrain types are thought to be extensive on Mars, including the fluvial deposits of the Circum-Chryse outflow channels (e.g. [11], [12], [13], [14]) and Athabasca Valles [15], the fluvio-lacustrine sediments of Utopia Planitia's floor (e.g. [16], [17]), bouldery surfaces of potential rock glaciers and protalus lobes in Candor Chasma [18] and moraine-like features in the Deuterolinus area [19]. Each of these terrain types may contain different water ice contents.

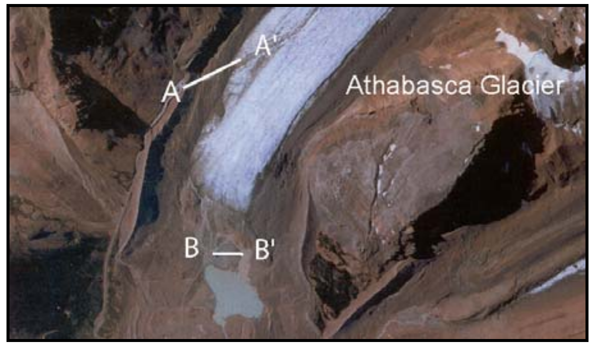

Figure 1. Aerial view of the terminus of Athabasca Glacier, Jasper National Park, Alberta, Canada [20]. The two white lines represent the two transects acquired with the GPR and CCRI systems.

Methodology: The resolution and penetration depth of GPR varies according to the antenna frequency, transmitter power and subsurface conditions. In order to optimize the ability to detect subsurface features, we used two GPR systems: the Pulse EKKO 100 (with 50 MHz and 100 MHz antennas) and the Noggin Plus (250 MHz) manufactured by Sensors and Software Inc. Electrical resistivity data was acquired using a OhmMapper CCRI system manufactured by Geometrics. Surveys were conducted along transects at two sites: a) the eastern lateral moraine of the Athabasca glacier (A-A') (fig.1), b) the outwash plain in front of the glacier (B-B') (fig.1).

GPR: Ground penetrating radar sends short pulses of EM energy into the ground and measures the energy reflected back (as a function of time). Although GPR shows reflections occuring from a variety of interfaces (e.g. thermal, moisture and structural) due to dielectric constant interfaces, the depth of penetration is reduced when electrically conductive sediments are present at the surface.

CCRI: Unlike traditional resistivity systems that employ electrodes planted in the ground, the OhmMapper consists of a transmitter and a set of receivers (up to 5) with coaxial antennas strung in series along a single cable (fig. 2) which is pulled along the ground either by a person (fig.2) or by a vehicle. The transmitter capacitively generates an electrical field within the ground and the receiver measures voltage differences as the system is pulled along the ground. Depth of penetration is determined by the array geometry and the resistivity of the subsurface material.

Figure 2. Person pulling the OhmMapper on the outwash plain.

Results: On the outwash plain, the GPR delineates sedimentary structures associated with glacio-fluvial and glacio-lacustrine sediment deposition. In contrast, the OhmMapper shows the bulk variations in sedimentary changes, including the location of an area where the bedrock rises near the surface.

On the moraine, the GPR profile shows a high amplitude laterally coherent reflection representing the base of the sediment cover over glacier ice. High concentrations of reflections near the glacier margin are interpreted as sedimentological changes and possibly representing zones of higher water content. The CCRI profile outlines an area of high resistivity (~250,000 Ohm.m) in the area of buried glacier ice.

Discussion and implications for Mars: The use of GPR in terrestrial environments has proven very successful for mapping ground ice. However GPR interpretation is usually undertaken in combination with subsurface verification methods such as coring and excavations. On Mars, however, these types of subsurface verification may not be viable. Capacitively-coupled resistivity imaging does not provide the resolution that GPR offers, however, it may offer the subsurface material verification required for detailed GPR interpretation.

Preliminary results show that GPR and CCRI techniques effectively complement each other by resolving different characteristics of the subsurface. While GPR clearly showed the subsurface structures and interfaces, CCRI provided diagnostic information about the electrical properties of the subsurface ice and sediment.

With the recent development of more complex inversion software, CCRI is able to produce two- and three-dimensional resistivity images of the subsurface, similar to GPR, thus improving the reliability of interpretations. As a result, a more comprehensive picture of the subsurface stratigraphy and its composition can be achieved. Additionally, both systems can be used on different types of surfaces thus increasing their versatility.

The development of GPR has indeed improved the capabilities of this technique during the past two decades and is likely going to be an integral part of future Mars missions. However, the combination of GPR and CCRI techniques could yield significantly more information concerning the availability of water ice in the Martian subsurface than GPR alone. The ability to identify and map near-surface ground ice as well as the possibility of quantifying ground ice volumes using GPR and CCRI imaging would prove beneficial to the continuing exploration of Mars, including the selection of future landing sites.

References: [1] Boynton W. V. et al. (2002) *Science, 29*6, 81 – 85. [2] Feldman W. C. et al. (2004) *JGR, 109*, E09006. [3] Mitrofanov I. et al. (2002) *Science, 297*, 78-81. [4] Stewart R. (2003) *Recorder*, *28,* 5-9. [5] Grimm R. E. (2003) *JGR*, *108*, 8037. [6] Arcone S. A. et al. (2002) *JGR*, *108*, 5108. [7] Berthelier J. J. et al. (2005) *JRL*, *32*, L22305. [8] Grant J. A. et al. (2003) *JGR*, *108*, 8024. [9] Heggy E. et al. (2001) *Icarus*, *154*, 244-257. [10] Leuschen C. et al. (2003) *JGR*, *108*, 8034. [11] Carr M. H. (1996) *Oxford Univ. Press, New York*. [12] Chapman M. G. and Kargel J. S. (1999) *JGR*, *104*, 8671-8678. [13] Jöns H. P. (1985) *LPS*, *XIV*, Abstract # 1985. [14] Lucchitta B. K. et al. (1986) *JGR*, *91*, E116-E174. [15] Burr D. (2005) *Geomorphology*, *69*, 242-252. 16] Chapman M. G. (1994). *Icarus*, *109*, 393-406. [17] McGill G. E. (2001) *GRL*, *28*, 411-414. [18] Whalley W. B. and Azizi F. (2003) *JGR*, *108*, 8032. [19] Head J. W. et al. (2005) *LPS XXXIV*, Abstract # 1257. [20]. Kucera E. R. (2002) *Report to Brewster Transport. Tour.*, 57p.